Calculation of Electromagnetic Forces for Magnet Wheels

Kokichi Ogawa and Yoko Horiuchi
Department of Production Systems Engineering, Oita University
700 Dannoharu, Oita, 870-11, Japan

Nobuo Fujii
Department of Electrical and Electronics Systems Engineering, Kyushu University
6-10-1 Hakozaki, Fukuoka, 812-81, Japan

Abstract - **The characteristics of magnet wheels for magnetic levitation and linear drives are investigated by using a three-dimensional computer simulation. Magnet wheels levitate by revolving permanent magnets over a conducting plate, in which the eddy currents are induced. The thrust is also produced by making the torque unbalance. This paper deals with the "partial overlap type" magnet wheels, producing the lift force and the thrust. The magnetic flux density and eddy currents are examined for the 4-pole and the 2-pole structures.**

I. Introduction

Magnet wheels, which can produce the repulsive type lift force by revolving the permanent magnets over the conducting plate, can levitate even in a standstill condition[1]-[3]. Two types of magnet wheels have been proposed to obtain the thrust utilized for linear drive. One is the "tilt type", in which revolving magnets are tilted against the surface of the conductor and the other is called the "partial overlap type"in which the rotator locates over the edge of the conductor. Especially, the latter type produces the additional lateral force which may be used for guidance. The three components of forces depend on the amount of displacement, defined as an important parameter in this configuration.

In this paper we describe the electromagnetic forces of magnet wheels calculated by using three-dimensional numerical analysis. In the discretization process of integral equations, the 2nd order interpolation function is used along the direction of flux penetration in order to take into account the skin effect. The characteristics at some displacements are investigated for the models of 4-pole and 2-pole magnet wheels.

II. Analysis

The characteristics of the "partial overlap type" magnet wheel depend on the displacement d_y, which is defined as the distance from one edge of the conductor to the center of the revolving magnets. The 4-pole construction and the definition of the displacement are illustrated in Fig.1.

Applying the vector Green's theorem to this model, the integral equation is obtained.

$$c_i \boldsymbol{A}_i = \int_{S_1} \frac{\mu_0 \boldsymbol{K}_m}{4\pi r} dS + \int_V \frac{\mu_0 \sigma}{4\pi r}\left(-\frac{\partial \boldsymbol{A}}{\partial t} - \nabla\phi\right)dV + \int_{S_2} \frac{\boldsymbol{r}}{4\pi r^3} \times (\boldsymbol{A} \times \boldsymbol{n})dS + \int_{S_2} \frac{\boldsymbol{r}}{4\pi r^3}(\boldsymbol{A} \cdot \boldsymbol{n})dS \quad (1)$$

where the region S_1 corresponds to the permanent magnets which are represented by the surface current $\boldsymbol{K}_m$, The region S_2 means the yoke with infinite permeability. The normal component of flux density on the air region of the boundary is neglected in this case. The rotator is assumed to revolve at a constant speed, and its position which is represented in the surface current term of (1) is different at every sampled time. The effect of motion is included in the term of time derivative. The region V indicates the non-magnetic conducting plate with the conductivity σ. In the conductor, the continuity of the eddy current is represented as follows:

$$\int_V \nabla N_i \cdot \sigma\left(-\frac{\partial \boldsymbol{A}}{\partial t} - \nabla\phi\right)dV = 0 \quad (2)$$

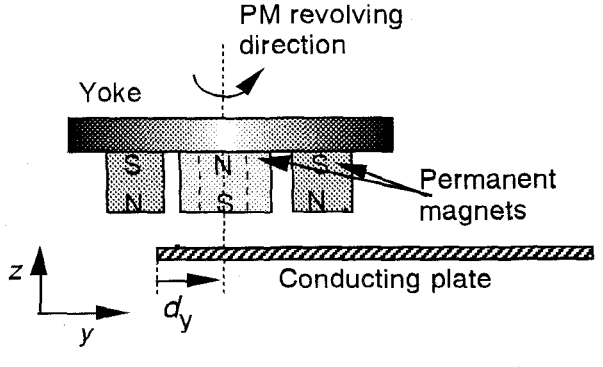

Fig.1 Schematic diagram of 4-pole magnet wheel.

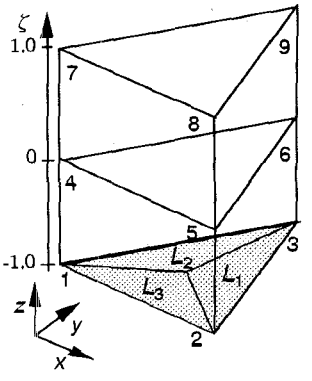

Fig.2 9-noded element and localized coordinates.

0018-9464/97$10.00 © 1997 IEEE

In the discretization process of these equations, the 9-noded element is used to take into account the skin effect. The 1st order interpolation function is used in the xy-plane facing the pole faces and the 2nd order interpolation function is used in the direction of flux penetration. The triangular linear element is used in the other area. The magnetic vector potential **A** and the scalar potential ϕ in the element of Fig.2 are expressed as follows:

$$A=\sum_{i=1}^{9} N_{ie}A_{ie} \tag{3}$$

$$\phi=\sum_{i=1}^{9} N_{ie}\phi_{ie} \tag{4}$$

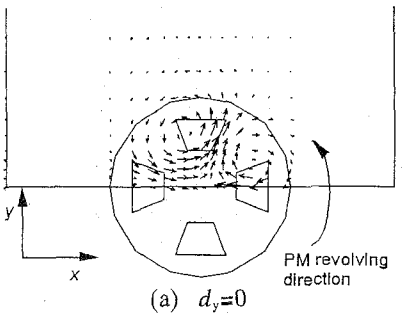

(a) d_y=0

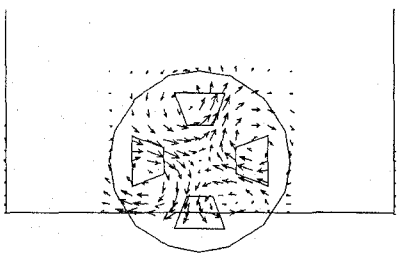

(b) d_y=60mm

Fig. 3 Eddy current on the upper surface of a conducting plate for 4-pole magnet wheels.

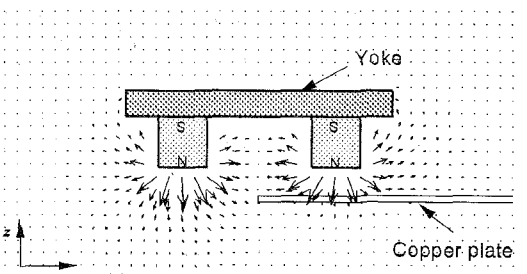

(a) d_y=0

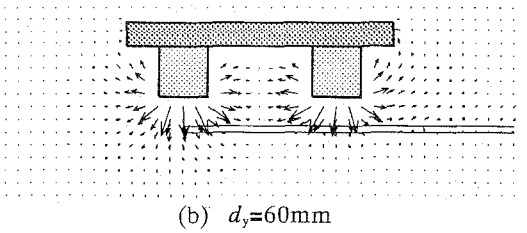

(b) d_y=60mm

Fig.4 Magnetic flux density in a cross section of yz-plane for 4-pole magnet wheels.

Its interpolation function N_{ie} is defined as

$$N_{ie}=\frac{1}{2}\xi(\xi-1)L_i \tag{5}$$

$$N_{(i+3)e}=(1-\xi)(1+\xi)L_i \tag{6}$$

$$N_{(i+6)e}=\frac{1}{2}\xi(\xi+1)L_i \tag{7}$$

for i=1, 2, 3.

Ⅲ. Numerical Results

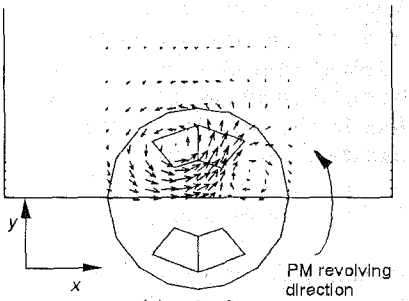

(a) d_y=0

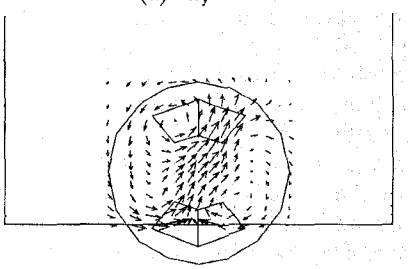

(b) d_y=60mm

Fig. 5 Eddy current on the upper surface of a conducting plate for 2-pole magnet wheels.

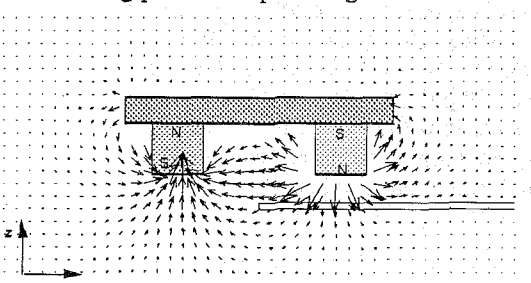

(a) d_y=0

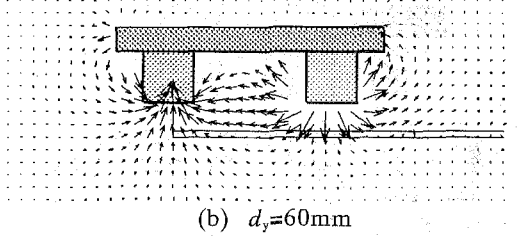

(b) d_y=60mm

Fig.6 Magnetic flux density in a cross section of yz-plane for 2-pole magnet wheels.

The computed results for the 4-pole and the 2-pole magnet wheels for some displacements are shown in this section. The eddy current distributions for the 4-pole construction are illustrated in Fig.3, in which the displacement d_y is 0 and 60mm respectively. The permanent magnet has the height of 40mm and the cross section width of 38mm, long side of 58mm and short side of 30mm. The yoke has 20mm height and 210mm diameter. Spacing by mechanical clearance of 20mm from the pole faces of magnets, the copper conducting plate with thickness of 5mm is located. The rectangular copper plate has 450mm×450mm area. It has sufficient width that permits to neglect the effect of the other edges except the operating edge under rotator. In the figure at the displacement d_y=0, the loop of eddy current is distorted remarkably and restricted by the existence of the edge compared with that at d_y=60mm.

The magnetic flux density vector in the x=0 plane is indicated in Fig.4, in which the rotator position corresponds to that in Fig.3. The magnetic flux passes from the north-pole of the magnet in airgap side to the south-pole of other two magnets separating perpendicular to yz-plane . Some amount of magnetic flux goes through the conducting plate because the thickness of the copper conductor is 5mm and it is thin. If larger lift force is needed, thicker conductor will be better.

The eddy currents for the 2-pole magnet wheels at d_y=0 and d_y=60mm are shown respectively in Fig.5. As the size of the eddy current loop gets larger than that in Fig.3, it becomes sensitive to the existence of the edge. The direction of the eddy current under the rotator in Fig. 5(a) is bent by the edge. The current near the edge flows almost parallel to the edge.

The magnetic flux indicated in Fig.6 passes from the north-pole to the south-pole of the other magnet in the same yz-plane, but large amount of leakage flux which does not link to the conductor exists. If the produced flux is defined as that at 2mm distance from the pole face, and the flux linkage is defined as that on the surface of the secondary plate, the ratio of leakage flux to the produced flux is 77% at d_y=0 and 60% at d_y=60mm respectively.

The instantaneous waveforms of the electromagnetic forces for the 4-pole constructions are indicated in Fig.7. The pulsation of lift force is related to the area of pole faces overlapping the conductor. But, the thrust scarcely pulsates at any displacement.

Waveforms of forces for the 2-pole magnet wheels are indicated in Fig.8. The lift force at the revolving angle of 90 degs. decreases remarkably as the little amount of pole face overlaps the conductor, and the pulsation grows large. One way of suppressing the pulsation may be to arrange some more magnets along the circumference of the rotator. Comparing with the 4-pole arrangements, the 2-pole construction produces the large lift force, thrust and lateral force in a range of positive values of displacement.

The lift force density distributions are illustrated in Figs. 9 and 10. The lift force is mainly produced in the conductor under the magnets in the 4-pole, and that in the 2-pole magnet wheel arises around the center of the rotator because the flux goes across the revolving axis.

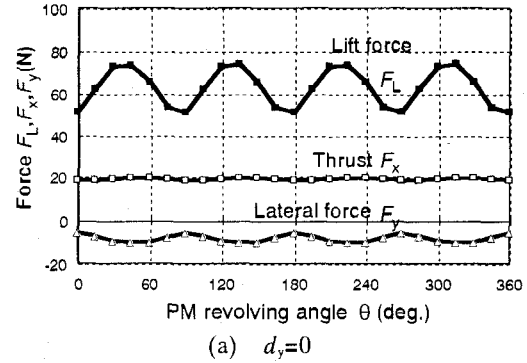

(a) d_y=0

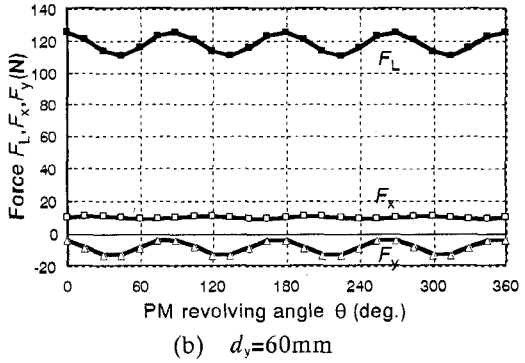

(b) d_y=60mm

Fig.7 Instantaneous waveforms of forces for 4-pole magnet wheels.

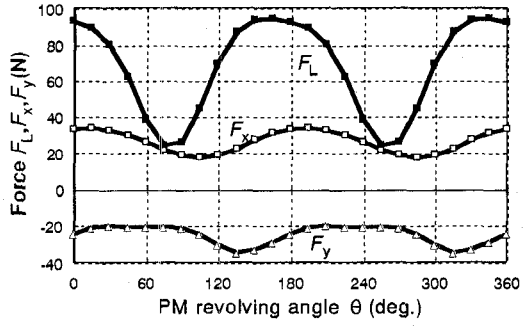

(a) d_y=0

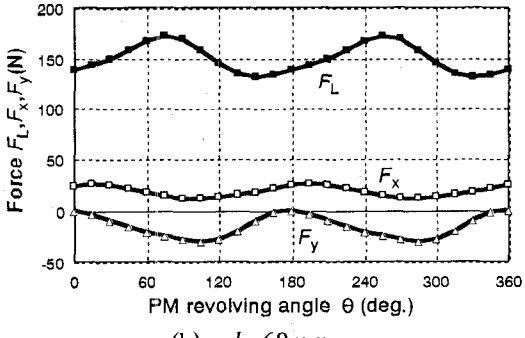

(b) d_y=60mm

Fig.8 Instantaneous waveforms of forces for 2-pole magnet wheels.

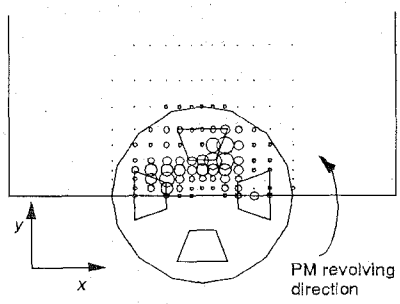

(a) d_y=0

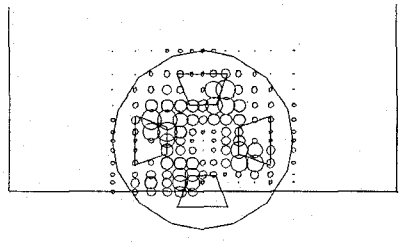

(b) d_y=60mm

Fig. 9 Lift force on the upper surface of a conducting plate for 4-pole magnet wheels.

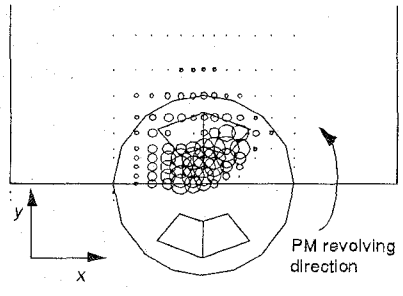

(a) d_y=0

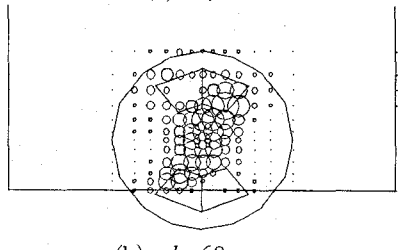

(b) d_y=60mm

Fig.10 Lift force on the upper surface of a conducting plate for 2-pole magnet wheels.

Figures 11 and 12 indicate the average forces versus displacement. The solid line and the broken line, in which the conductors are discretized by linear elements, neglect the skin effects. The symbols F_{x2}, F_{y2} and F_{L2} mean results calculated by using the 2nd order interpolation function in the direction of flux penetration. As the thickness of the conductor is thin as 5mm, the difference due to the skin effect is small.

By comparing the 4-pole and the 2-pole structures, the thrust for the 2-pole magnet wheel is superior in the range

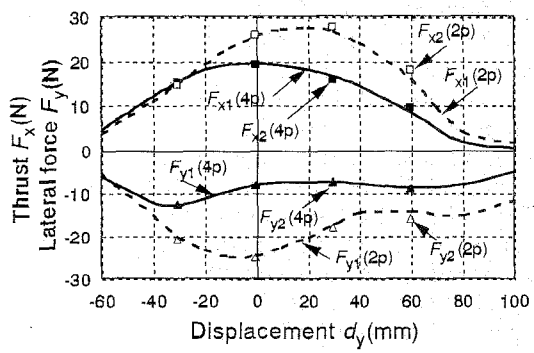

Fig. 11 Thrust and lateral force versus displacement for 4-pole and 2-pole magnet wheels.

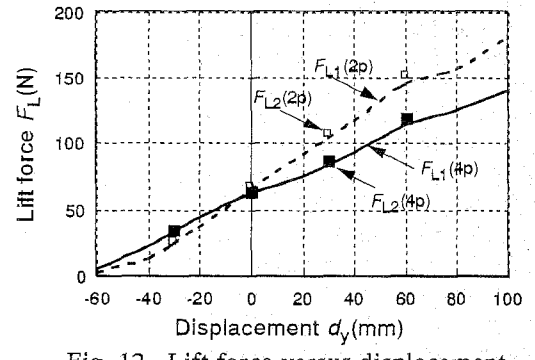

Fig. 12 Lift force versus displacement for 4-pole and 2-pole magnet wheels.

of $d_y \geqq$-20mm and the lateral force is also superior in the range of d_y. When d_y has a positive value, lift force for the 2-pole is superior to the 4-pole. When the volume of the magnet is same in both configurations, the 2-pole magnet wheel produces the higher force density.

Ⅳ. Conclusions

The effects of the displacement for the 2-pole and the 4-pole magnet wheels are investigated by using numerical calculation. Though the 2-pole structure is sensitive to the existence of the conductor edge, it produces larger thrust and larger lateral force. The pulsation of the lift force appears remarkably at the small displacement for the 2-pole structure. For the 4-pole construction the pulsation of the thrust scarcely exists at any displacement.

References

[1] N. Fujii, K. Naotsuka, K.Ogawa and T. Matsumoto, "Basic characteristics of magnet wheels with rotating permanent magnets," IEEE IAS 20th Annual Meeting, pp.203-209, Oct. 1994.

[2] N. Fujii, K. Ogawa and T. Matsumoto, "Revolving Permanent Magnet Type Magnet Wheels," Trans. IEE Japan, vol. 115D, 3, pp. 319-326, Mar.1995.

[3] N. Fujii, K. Ogawa and K. Naotsuka, "Analysis for Static Characteristics of Magnet Wheels," Trans. IEE Japan, vol. 115D, 3, pp.327-335, Mar.1995.